High-spin and low-spin states in Invar and related alloys

V. L. Moruzzi
IBM Research Division, Thomas J. Watson Research Center, P.O. Box 218, Yorktown Heights, New York 10598
(Received 9 December 1988; revised manuscript received 8 May 1989)

Total-energy band calculations that show the coexistence of a high-spin and low-spin state in fcc transition metals and alloys are presented. The energy difference between the two states is shown to be a function of the electron concentration and to vanish at 8.6. At larger electron concentrations the low-temperature state is the high-spin state, and the thermal expansion is shown to pause at a system-dependent characteristic temperature. At lower electron concentrations the low-temperature state is the low-spin state, and enhanced thermal expansion is expected. An analysis that leads to a qualitative understanding of the thermal properties of Invar and that implies a connection with martensitic transformations and spin glasses in related alloys is presented. For Invar a magnetic collapse from the high-spin to the low-spin state at a pressure of 55 kbar is predicted.

I. INTRODUCTION

The problem of the anomalous thermal expansion of Fe-Ni alloys has attracted considerable attention since the discovery[1] of Invar almost a hundred years ago. Although it was recognized from the beginning that the low room-temperature thermal expansion must be related to complicated magnetic effects, Weiss's proposal[2] of the existence of two γ states offered the first serious explanation of this unusual effect. The two discrete states in the Weiss model correspond to individual iron sites which are assumed to have different local moments and volumes. Recently, we presented[3] conventional spin-polarized band calculations which imply the existence of a nonmagnetic state lying just above the ferromagnetic state in Invar. More recently, we have shown[4] that total-energy fixed-spin-moment band calculations yield an energy versus volume curve displaying a low-spin state centered at low volumes, and a high-spin state centered at high volumes, with the low-spin state at approximately 1 mRy (150 K) above the high-spin state. We further showed that the low-temperature thermal expansion could be explained in terms of a thermal population of the higher energy low-spin state and that the initial negative thermal expansion is probably due to the coexistence of a third, antiferromagnetic state with a volume intermediate between the low-spin and high-spin volumes and an energy a few tenths of a mRy above the high-spin energy.

Here we extend our earlier work and study the thermal properties of a range of Fe-Ni and related alloys. In Sec. II we briefly describe the fixed-spin-moment procedure used in our work and show that it yields low-spin and high-spin states and that the energy difference between the two states vanishes at a critical concentration of 8.6 electrons. In Sec. III we show that Invar properties, characterized by a pause in the thermal expansion, must occur at successively higher temperatures as the electron concentration increases. In Sec. IV we show that "anti-Invar" behavior, characterized by an enhancement (rather than a pause) in the thermal expansion, is expected and that this behavior occurs at successively higher temperatures as the electron concentration decreases. We propose a direct connection between these characteristic anti-Invar temperatures and martensitic transformations. In Sec. V we show that complex magnetic properties, including dilute ferromagnetic and spin-glass behavior are expected at low temperatures for concentrations near the critical value of 8.6 electrons. We also show in Secs. III and IV that, at a pressure of 55 kbar and at low temperatures, Invar is expected to undergo a magnetic collapse from the high-spin to the low-spin state, and that Invar should exhibit anti-Invar behavior (enhanced thermal expansion) at pressures exceeding 55 kbar.

II. FIXED-SPIN MOMENTS

Our current results are based on total-energy augmented-spherical-wave band calculations[5] utilizing the fixed-spin-moment procedure.[6] Conventional band calculations with total energy capabilities generally treat the volume V as an independent parameter and find the binding curve of the system. The resulting volume dependence of the total energy $E(V)$ generally displays only one stable solution, at the energy minimum where $dE/dV=0$. The volume corresponding to the minimum is the equilibrium volume, V_0. All other points on the binding curve simply correspond to the total energy of the system with the volume constrained to the given value by an effective external pressure, $P=-dE/dV$. With the fixed-spin-moment procedure, we have the added flexibility of treating the amplitude of the magnetic moment, M, as a second independent parameter and finding, at a given volume, the total energy versus moment curve. The resulting $E(M)$ curve displays minima at different magnetic moment values. As in the former case, the only stable solutions correspond to moment amplitudes at local minima where $dE/dM=0$. All other points on the $E(M)$ curve correspond to the total energy of the system with the moment constrained to the given value by an effective external magnetic field, $H=dE/dM$. In general, a given system will have different $E(M)$

curves at different volumes.

Fixed-spin-moment band calculations show[7] that all transition metals have $E(M)_V$ curves with stable solutions at $M=0$ for low volumes, and with stable solutions at a finite M value at large volumes. Thus, all transition metals are nonmagnetic at sufficiently low volumes, and become magnetic at sufficiently high volumes. This general result is not surprising when it is considered that, at low volumes the transition-metal d bands are spread over a large energy range and are incapable of supporting magnetic behavior, while at large volumes the free-atom limit and moments consistent with Hund's rule and the atomic ground-state configuration must be approached.

The fixed-spin-moment procedure which we use is ideal for studying the details of this transition from nonmagnetic behavior. Depending upon the system, it is found that the transition can be either first order or second order. In the case of a first-order transition, $E(M)_V$ curves displaying two stable ($H=0$) solutions, one at $M=0$ and one at a finite M value, are found over a limited volume range. That is, there is a volume range where the system can be either nonmagnetic or magnetic. The zero-field energy versus volume for such a system must be represented as two separate but crossing branches, with the overlap defining a coexistence region. In this case, the moment versus volume is discontinuous. At the branch crossing, the moment can be zero or have a finite value with no change in the total energy of the system. We refer to this as a magnetic instability and to the nonmagnetic and magnetic branches as low-spin and high-spin branches. The low-spin designation can refer to either nonmagnetic or to low-spin solutions which are found for complex systems involving more than one atomic species.

Note that fixed-spin-moment calculations differ in detail from conventional band calculations. Our original[3] evidence for the coexistence of nonmagnetic and ferromagnetic states in Invar is based on two conventional calculations; a (constrained) nonmagnetic calculation, and a spin-polarized calculation. In our more recent work,[4] a single fixed-spin-moment band calculation yields both states simultaneously, and shows that they can coexist over a limited volume range.

Additional band-theoretical evidence for the existence of high-spin and low-spin states in transition metals is based on total-energy fixed-spin-moment calculations for iron[8] and cobalt constrained to an fcc unit cell. The basic calculations result in total energy contours in magnetic moment and volume space. The zero-field results, defined by loci of points at which dE/dM vanishes ($H=0$) are reproduced in Fig. 1 and Fig. 2, respectively, where we show E and M versus the Wigner-Seitz radius, r_{WS}. Here, the volume is given by $V=(4\pi/3)r_{WS}^3$. In both systems, the behavior is nonmagnetic at low volumes and ferromagnetic at high volumes. The transition from nonmagnetic to magnetic behavior is first order, as evidenced by the discontinuity in the magnetic moment and the two separate but crossing branches of the total energy. As shown, we find that the low-energy state is nonmagnetic for iron and ferromagnetic for cobalt. The higher-lying ferromagnetic state for iron and nonmagnetic state for

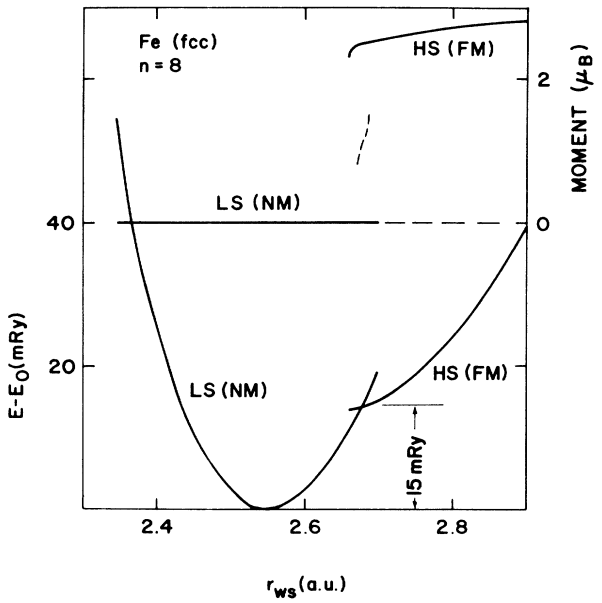

FIG. 1. Total-energy fixed-spin-moment results for iron constrained to a one atom fcc unit cell showing a magnetic instability at an expanded volume and at an energy of 15 mRy. The dashed magnetic moment curve in the upper panel corresponds to an unimportant low-spin solution persisting over a limited volume range.

cobalt have minima at approximately 15 and 10 mRy, respectively.

Figure 1 (and 2) represents the total electronic energy as a function of the scale of the rigid lattice, and therefore does not account for temperature-dependent lattice vibrations. That is, the figure gives a *macroscopic* view of the behavior of the system of atoms on the rigid lattice. In the strictest sense, the figures does not even apply for zero temperature because zero-point lattice vibrations are not considered. A detailed understanding of thermal ex-

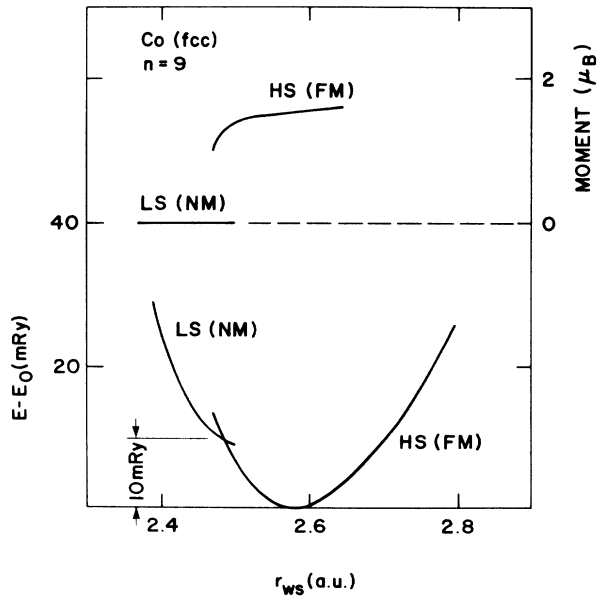

FIG. 2. Total energy fixed-spin-moment results for cobalt constrained to a one atom fcc unit cell showing a magnetic instability at a compressed volume and at an energy of 10 mRy.

pansion requires the evaluation of the thermal evolution of the free energy; a difficult task for systems exhibiting magnetic instabilities because of the complicated volume dependence of the local moments. The approximate thermal behavior of the system, however, can be inferred from binding curves such as Figs. 1 and 2. In general, electronic-structure calculations yield binding curves that show positive anharmonicity. That is, they are skewed towards higher volumes. At elevated temperatures, the *microscopic* effective local volume associated with an individual atom can have wide excursions from that given by the rigid lattice minimum. Positive anharmonicity implies a tendency for the atom to have, on average, a larger effective local volume at successively higher temperatures. It is this positive anharmonicity and resulting increase in effective local volumes that leads to thermal expansion of simple metals. The existence of the higher-energy nonmagnetic, low-volume branch in Fig. 2, introduces an effective negative anharmonicity, a tendency towards lower effective local volumes, and a tendency to contract. Conversely, the existence of the higher-energy high-spin, high-volume branch in Fig. 1 introduces an additional positive anharmonicity and tendency for greater than normal expansion.

The difference between the energy minimum, E_0, and the minimum energy for the higher-lying state is a measure of the temperature required to excite the upper state. Since 1 mRy is approximately 150 K, the higher-lying states for the two systems represented in Figs. 1 and 2 can only be excited at temperatures in excess of a thousand degrees. Hence, thermal expansion anomalies would only be apparent at very high temperatures where they would be difficult to detect. That is, the instabilities are well beyond the "normal" thermal range. Although beyond the thermal range, Wassermann[9] proposed that our calculated magnetic instability for fcc iron may play a crucial role in the thermal expansion of Invar.

In general, the source of the magnetic instabilities is a high density-of-states at the Fermi energy, which is a consequence of d-band filling. Therefore, the details of the instability and the differences in energy corresponding to the minima of the two states are a function of the number of valence electrons. As is evident from a comparison of Fig. 1 and Fig. 2, the difference between the nonmagnetic energy minimum and the ferromagnetic energy minimum $\Delta E = E_{\rm NM} - E_{\rm FM}$ changes sign in going from iron with eight electrons to cobalt with nine electrons. Based on these two systems only, a linear interpolation shown in Fig. 3 implies that an fcc system with 8.6 valence electrons per atom would have zero energy difference. In this case, both states would be thermally accessible even at the lowest temperatures, and temperature-dependent lattice vibrations would strongly influence local magnetic moments. We note that Invar is the fcc Fe-Ni alloy with 35% nickel containing approximately 8.6 valence electrons per atom. The agreement between this crude linear interpolation based on two elemental systems and the valence electron count for Invar may be fortuitous. In particular, we note that because of hybridization effects, compounds (i.e., ordered Fe_3Ni to be discussed later) would not fall on the straight line

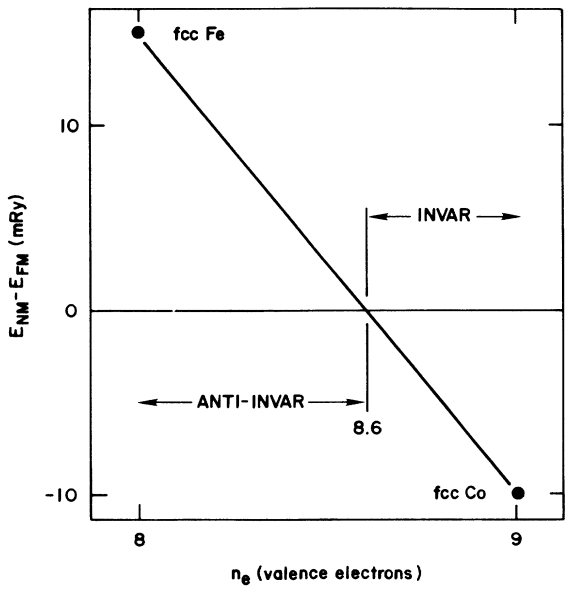

FIG. 3. Difference between the ferromagnetic and nonmagnetic energy minima for fcc iron and fcc cobalt. A linear interpolation implies a zero energy difference for 8.6 valence electrons.

shown in Fig. 3. The figure gives a crude rigid-band estimate of the expected energy difference between the nonmagnetic and magnetic branches.

For electron concentrations greater than 8.6, the energy versus volume curves are expected to resemble those of fcc cobalt, with the nonmagnetic state at a higher energy than the ferromagnetic state and with the resulting instability at lower volumes than the volume corresponding to the absolute energy minimum. In this case, ΔE is negative and decreases (becomes more negative) as the number of electrons increases towards the cobalt value. We will show that systems in which this energy difference is negative will exhibit a "pause" in the thermal expansion, correspondingly low coefficients of expansion at system-dependent temperatures, and Invar-typical behavior.

For electron concentrations less that 8.6, the energy versus volume curves are expected to resemble those of fcc iron, with the ferromagnetic state at a higher energy than the nonmagnetic state, and with the resulting instability at larger volumes than the volume corresponding to the absolute energy minimum. In this case, ΔE is positive and increases as the number of electrons decreases towards the iron value. We will show such systems will exhibit what we refer to as anti-Invar behavior with "enhanced" thermal expansion (large volume changes) at successively higher temperaturess as the number of electrons decreases or as we approach iron-rich alloys in the Fe-Ni system. We propose that, upon cooling, the expected large volume changes trigger a martensitic transformation from a metastable γ phase to mixed $\gamma+\alpha$ phases at temperatures which depend upon the electron concentration.

Simple metals which do not exhibit magnetic instabilities have binding curves like that shown schematically in

Fig. 4(a). The energy represented in such binding curves is the total *electronic* energy of the system as a function of the scale of the rigid lattice, and therefore does not account for temperature-dependent lattice vibrations. However we have shown[10] that, by using a Debye-Grüneisen approximation, we can account for lattice vibrations and effectively extend our band calculations to finite temperatures. We showed that Debye temperatures and Grüneisen constants implicit in calculated rigid-lattice binding curves are sufficient to define the energy and entropy due to lattice vibrations and the resulting thermal evolution of the free energy. The Debye-Grüneisen analysis yields the volume versus temperature directly from first-principles band calculations within the local-density-approximation with the atomic number as the only input. As shown schematically in Fig. 4(e), it is found that the rate of expansion approaches zero at the zero-temperature limit, and approaches a constant value at high temperatures. An extrapolation of the linear high-temperature behavior back to zero temperature yields the rigid-lattice volume, V_0, derived from band calculations. The difference between the volume at zero temperature, and the rigid-lattice volume is simply a zero-point energy effect. We will use this observation to discuss the thermal properties of Fe-Ni alloys. The temperature derivative of the volume versus temperature behavior shown in Fig. 4(e) yields the normal coefficient of the expansion curve shown schematically in Fig. 5(a).

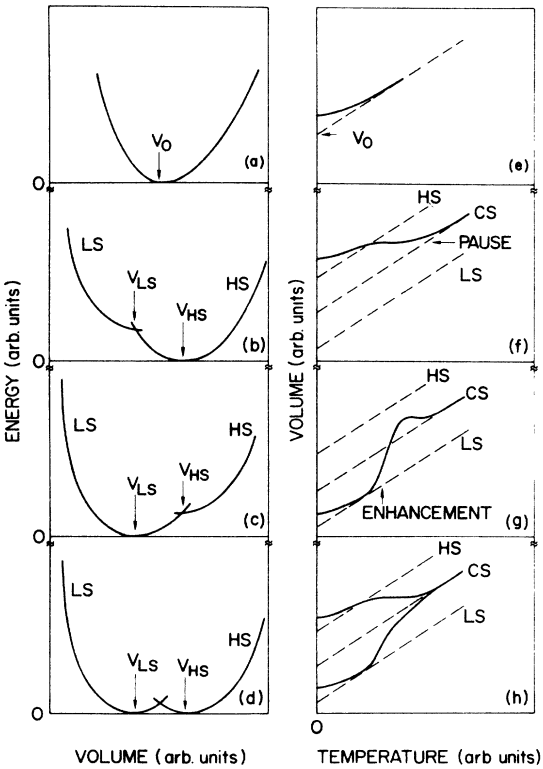

FIG. 4. Schematic total energy vs volume for a simple metal (a), an Invar system (b), an anti-Invar system (c), and a spin glass (d). The corresponding volume vs temperature behavior are shown in (e), (f), (g), and (h). The rigid-lattice equilibrium volume for simple metals is labeled V_0. LS and HS refer to the low-spin and high-spin states, and CS refers to composite low-spin, high-spin behavior.

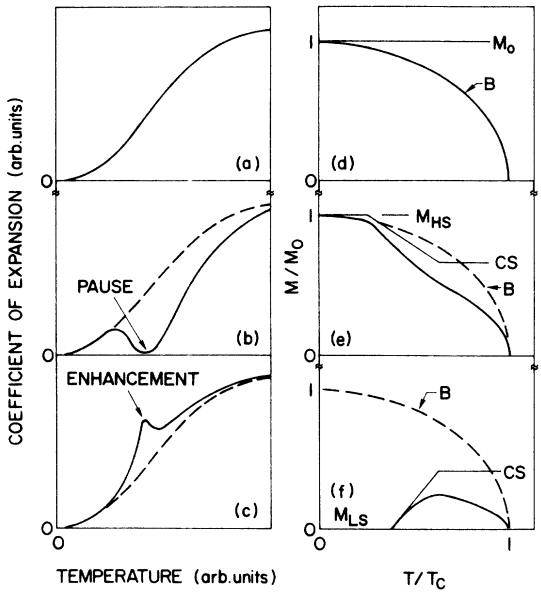

FIG. 5. Schematic coefficient of expansion curves for a simple metal (a), an Invar system (b), and an anti-Invar system (c). The corresponding magnetic behavior is shown in (d), (e), and (f). Brillouin behavior is labeled B, and composite low-spin, high-spin behavior is labeled CS. M_0 is the amplitude of the local moment at V_0 for a simple magnetic metal. M_{HS} and M_{LS} are the amplitudes of the local moments at the high-spin and low-spin lattice volumes, respectively. The amplitude of the local moments in (e) and (f) is shown by the straight line segments with sharp breaks. These breaks are expected to be rounded off by thermal effects.

It is well established that the amplitudes of local moments in magnetic metals (with no magnetic instabilities) are relatively independent of temperature, and that they persist through the Curie temperature. The magnetization, on the other hand, is a consequent of spin disorder and is expected to follow a Brillouin behavior, dropping to zero at the system-dependent order-disorder Curie temperature as shown in Fig. 5(d).

III. INVAR

We will consider the ordered Fe_3Ni system to be a "model" Invar system even though we know that true Invar is chemically disordered and has a slightly different stoichiometry. Fixed-spin-moment band calculations on this system yield the zero-field results shown in Fig. 6. As in the case of fcc iron and cobalt, we find that the total energy must be represented as two separate but crossing branches with a discontinuous magnetic moment at the crossing. The resulting instability occurs at a volume below the absolute energy minimum which corresponds to a high-spin state. Because this is a two component system, the situation is more complicated than the elemental fcc iron and cobalt cases. For Fe_3Ni, the lower volume branch corresponds to a low-spin state with small local

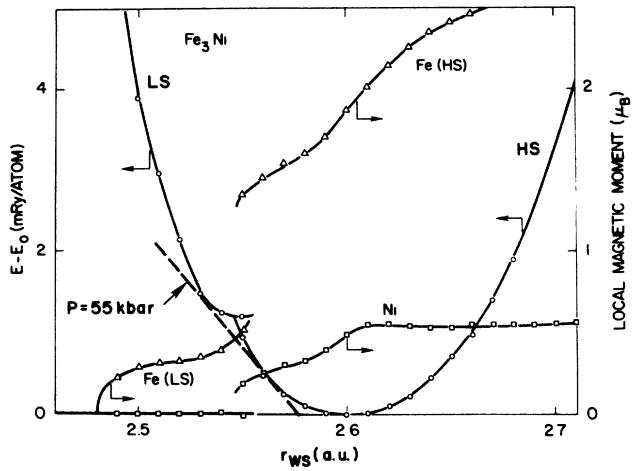

FIG. 6. Calculated total energy and magnetic moments versus r_{WS} for ordered Fe_3Ni showing a low-spin state centered at low volumes and a high-spin state centered at high volumes. The two states are the band-theoretical equivalent of the 2-γ states proposed by Weiss. At zero temperature, the two states are in equilibrium at the pressure represented by the common tangent or at 55 kbar.

moments on the iron sites and no moments on the nickel sites. The ferromagnetic branch corresponds to a high-spin state with local moments on both iron and nickel sites. The average magnetic moment corresponding to the low-spin and high-spin minima, M_{LS} and M_{HS}, are 0.4 and $1.6\mu_B$, respectively. Note that the low-spin state has an energy minimum that is only 1 mRy above the absolute energy minimum of the high-spin state and has a volume centered below that of the high-spin state at $r_{WS}=2.6$ a.u. Thermal excitation of this low-spin state will begin at thermal energies exceeding 1 mRy or at temperatures of approximately 150 K.

Figure 6 represents zero-field, rigid-lattice results. Temperature is not explicitly considered in the calculations, and no attempt is made to find the thermal evolution of the free energy as was done for simple metals.[10] The major goal of the present work is to give a *qualitative* understanding of the thermal expansion of Invar. For this purpose, it is sufficient to recognize that an energy of 1 mRy above the absolute energy minimum corresponds to a temperature of approximately 150 K and that, in general, increased energy differences imply higher temperatures.

As a consequence of lattice vibrations, the effective (microscopic) local volume of an individual atom is expected to have a progressively wider range of values as the temperature increases. At approximately 150 K, the effective local volume will tend to have (for a brief part of the cycle and for certain vibrational modes), a value corresponding to the low-spin, low-volume branch at $r_{WS}\simeq 2.55$ a.u. At still higher temperatures, this tendency towards lower volumes will increase and the system will tend to contract as the local moments collapse. That is, "normal" thermal expansion will tend to be inhibited because of the tendency of individual atoms to have lower effective local volumes while they undergo a collapse (longitudinal) in local moment.

Ignoring zero-point energy effects, the high-spin and low-spin states are in equilibrium at the pressure represented by the common-tangent line shown in Fig. 6 or at $P=-dE/dV=55$ kbar. Thus, at zero temperature and at pressures exceeding 55 kbar, we would expect magnetic collapse from the high-spin to the low-spin state in Invar. The pressure induced magnetic phase transition recently observed by Abd-Elmequid *et al.*[11] in Invar at 58 kbar is a direct experimental confirmation of the validity of our band calculations and of the theoretically predicted pressure for magnetic collapse shown in Fig. 6.

The high-spin and low-spin volumes indicated by the position of the minima in Fig. 6 are rigid lattice volumes. At temperatures below 150 K, only the high-spin state is occupied and the system is expected to expand like any other system and to have the high-spin rigid lattice volume corresponding to $r_{ws}=2.6$ a.u. At temperatures of about 150 K, population of the low-spin state which is centered at a lower volume begins. As a consequence, the normal high-spin expansion is interruped and there is a "pause" in the expansion. At temperatures well above 150 K, the system again expands like any normal system with composite high-spin, low-spin character. At these temperatures, the system has an effective rigid lattice volume that lies somewhere between that of the high-spin and that of the low-spin state, and is therefore *less than* the high-spin volume. We therefore summarize the Invar effect by the schematic energy versus volume curve shown in Fig. 4(b) and the volume versus temperature curve shown in Fig. 4(f). A temperature derivative of the curve shown in Fig. 4(f) yields the Invar-typical coefficient of thermal expansion curve shown in Fig. 5(b). Thus, the low room-temperature thermal expansion in Invar is a consequence of a pause in the expansion resulting from a population of the lower volume low-spin state in accordance with the Weiss proposal.

Note that, as the nickel composition and electron concentration increases, the energy difference between the high-spin and low-spin minima increases. Theory implies a corresponding increase in the temperature required to begin populating the low-spin state. This characteristic Invar temperature should have successively higher values with increasing nickel composition, as observed experimentally. At large electron concentrations (i.e., for cobalt), Invar behavior occurs only at temperatures where the normal thermal expansion is so large that the effect is difficult to resolve.

The magnetic behavior for Invar systems is complicated by the different thermal population of two different states. The expected behavior is shown schematically in Fig. 5(e). The low-temperature magnetic moment amplitude, M_0, is constant and corresponds to the moment at the high-spin minimum. That is, M_0 is equivalent to M_{HS}. At some system-dependent characteristic temperature, the *average* amplitude must decrease as the low-spin state begins to be populated; finally reaching a composite average at high temperatures. The magnetization is now expected to be influenced by this change in amplitude, and to exhibit a deviation from normal Brillouin behavior

as shown in the Fig. 5(e), and as found experimentally.[12]

As depicted in Fig. 5(e), the average amplitude of the local moment is temperature dependent. Here, the amplitude is shown as straight line segments with a sharp break from low-temperature high-spin behavior to a linear transition region and another sharp break to high-temperature composite behavior. Only the end points are meaningful. In particular, we expect the indicated sharp breaks to be rounded by thermal effects. In addition, the sharp order-disorder Curie temperature implied in the figure may actually be smeared because of the composite (high-spin and low-spin) behavior at these temperatures.

IV. ANTI-INVAR

The interpolation in Fig. 3 implies that at electron concentrations less than approximately 8.6, the low-spin state is lower in energy than the high-spin state as shown schematically in Fig. 4(c). In this case, the instability shifts to expanded volumes as for fcc iron. At low temperatures, only the low-spin state is occupied and the system expands accordingly. At some system-dependent characteristic temperature, population of the high-spin state, which is centered at a larger volume, begins. As a consequence, the system is expected to experience an additional increase in volume or an "enhancement" in the thermal expansion as shown in Fig. 4(g). At high temperatures, a composite high-spin, low-spin behavior with an effective rigid-lattice volume somewhere between that of the high-spin and that of the low-spin state is expected. Therefore, the composite rigid-lattice volume must be *greater than* the low-spin volume. We refer to this as anti-Invar behavior. The corresponding coefficient of expansion defined by the temperature derivative of Fig. 4(g) is shown in Fig. 5(c).

The expected magnetic anti-Invar behavior is shown in Fig. 5(f). In this case, the amplitude of the local moments at low temperatures correspond to the low-spin state. At some system-dependent characteristic anti-Invar temperature, the average amplitude must increase as the population of the high-spin state begins; finally reaching a composite average at high temperatures. Thus, the average amplitude of the local moments increases with increasing temperature and leads to a curious magnetization curve that also increases over a limited temperature range. Spin-disorder then leads to a falloff at still higher temperatures.

Experimentally, it is found[13] that Fe-Ni alloys with less than approximately 32% nickel undergo a martensitic transformation from the γ (fcc) phase, stable at high temperatures, to a mixed $\gamma+\alpha$ (bcc) phase at low temperatures. Thus, the interesting low-temperature behavior shown in Fig. 4(g), Fig. 5(c), and Fig. 5(f) is not normally realized for this alloy system. The transformation temperatures on cooling are found to vary from zero for the 32% nickel composition to 1180 K for pure iron. Moreover, the transformation temperatures are found to be much larger for the reverse transformation. Obviously, the γ phase is metastable at temperatures between the cooling and heating transformation temperatures. On cooling to this temperature range, the fcc atomic configurations are "frozen" in place and an atomic rearrangement is required for the system to assume the α phase. That is, there is an energy barrier preventing the transformation. However, at temperatures corresponding to the energy difference between the high-spin and low-spin state, the expected large volume changes at the enhanced thermal expansion region shown in Fig. 4(g) may help to induce the transformation. Thus, we propose that the $\gamma \rightarrow \gamma+\alpha$ (cooling) transformation temperature is directly related to the energy difference between the high-spin and low-spin states, and we identify this temperature with our characteristic anti-Invar temperature. In our theory, the energy of the instability is zero for an alloy near the Invar composition (8.6 electrons), increases as the nickel composition (and electron concentration) decreases, and goes to approximately 15 mRy for pure iron. This theoretically expected behavior agrees with the experimentally observed variation of martensitic transformation temperatures.

Although the pause in the thermal expansion due to the thermal population of low-volume low-spin states shown in Fig. 4(f) and Fig. 5(b) is well established for Invar-like transition-metal systems, there is little direct experimental evidence for the enhancement shown in Fig. 4(g) and Fig. 5(c). As we have noted, Fe-Ni alloys with low nickel concentrations exhibit martensitic transformations before anti-Invar effects become pronounced. In related transition-metal alloys, notably Fe-Ni alloys which contain manganese[14] to suppress the martensitic transformation, the occurrence of antiferromagnetism complicates the simple analysis depicted in Fig. 4 and Fig. 5. These antiferromagnetic systems also exhibit Invar-typical behavior with a pause in the thermal expansion. We suggest that in these antiferromagnetic Invar systems, our high-spin ferromagnetic state is replaced by an antiferromagnetic state which has a minimum at a *lower* energy than the low-spin state even for low nickel concentrations. The observed pause in thermal expansion is again due to a thermal population of the low-volume low-spin state. Thus, our interesting anti-Invar effects are suppressed along with the martensitic transformations. We note however that, under a constant pressure in excess of 55 kbar, Invar may exhibit anti-Invar behavior (or may undergo a martensitic transformation). As shown in Fig. 6 and verified experimentally,[11] the low-temperature state for Invar becomes the low-volume low-spin state for $P > 55$ kbar. At a characteristic temperature which depends upon the excess pressure (above 55 kbar), the higher volume high-spin state can be excited. Under these conditions, Invar is expected to exhibit anti-Invar behavior with enhanced thermal expansion as shown in Fig. 4(g) and Fig. 5(c), and with the curious magnetic behavior shown in Fig. 5(f).

Based on this theory, the behavior of Fe-Ni alloys with electron concentrations between 8 (iron) and 9 (FeNi or cobalt) is summarized in Fig. 7. For concentrations between 8.6 and 9, we expect the high-spin state to be favored at low temperatures, a pause in the thermal expansion, and Invar behavior with a characteristic Invar temperature T_{Inv} increasing with electron concentration. For concentrations between 8 and 8.6, we expect the

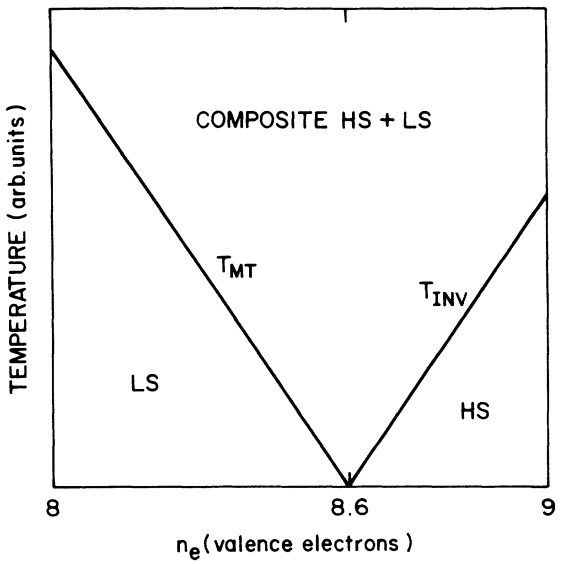

FIG. 7. Expected behavior for Fe-Ni alloys. Invar behavior occurs for electron concentrations between 8.6 and 9 where the high-spin state is fully occupied at low temperatures (high-spin state lower than low-spin state). Anti-Invar behavior occurs for electron concentration between 8 and 8.6 where the low-spin state is fully occupied at low temperatures (low-spin state lower than high-spin-state). The composite high-spin and low-spin region at high temperatures is indicated. Characteristic Invar temperatures are given by the line separating the high-spin and composite regions. Characteristic anti-Invar temperatures are given by the line separating the low-spin and composite regions. This latter temperature is identified as the martensitic transformation temperature.

low-spin state to be favored at low temperatures, an enhancement in the thermal expansion, and anti-Invar behavior with a characteristic temperature increasing with decreasing electron concentration. We identify this temperature with martensitic transformation temperature, T_{MT}. For temperatures above T_{Inv} and T_{MT}, we expect composite high-spin, low-spin behavior. The pure low-spin behavior in the anti-Invar region is not normally realized because of the transformation.

V. SPIN GLASSES

At low temperatures and at electron concentration of 8.6, we expect critical behavior. In this case, the high-spin and low-spin branches of the energy versus volume curves would ideally have minima at the same energy as shown in Fig. 4(d). However, these Fe-Ni alloys are chemically disordered and therefore have microscopic composition gradients and a corresponding variation in the energy versus volume behavior. That is, the energy difference between the low-spin and high-spin minima is not zero, but rather has a range of positive and negative values centered around zero. On a microscopic scale and at low temperatures, such a system should condense into Invar and anti-Invar droplets with *local* volumes varying with temperature as shown in Fig. 4(h). The system then consists of a matrix of droplets with a regular fcc crystallographic lattice but with very different magnetic behavior and with large internal stresses at the droplet boundaries. In the Fe-Ni system, the Invar droplets would have a high-spin local moment amplitude, while the anti-Invar droplets would have a low-spin local moment amplitude (or be nonmagnetic). The system would then exhibit complex magnetic behavior with the long-range magnetic order associated with Invar droplets disrupted by nonmagnetic anti-Invar droplets. Such a system might be described as a dilute ferromagnet.

We have shown[15] that fcc iron is expected to exhibit antiferromagnetic behavior. In addition, we have proposed[4] that antiferromagnetic behavior accounts for the initial (low-temperature) negative, thermal expansion of Invar. Therefore, anti-Invar droplets near the Invar composition may, in fact, be antiferromagnetic. At low temperatures, Invar should then exhibit coexisting antiferromagnetic and ferromagnetic properties, as observed experimentally by Zähres *et al.*[16] and by Miyazaki *et al.*[17] Under these conditions, Fe-Ni alloys near the Invar composition can be characterized as a matrix of antiferromagnetic and ferromagnetic droplets with spin-glass properties.

It is well known that martensitic transformations are suppressed and that antiferromagnetism is promoted in the anti-Invar region in quasibinary Fe-Ni alloys containing manganese, chromium, or vanadium. Fixed-spin-moment band calculations on fcc iron and manganese[18] show a clear tendency for antiferromagnetism at the Invar equilibrium volume. Experimentally, it is observed[14,19] that the alloy system, $Fe_{65}(Ni_{1-x}Mn_x)_{35}$, exhibits a magnetic phase diagram showing ferromagnetic and antiferromagnetic behavior at low- and high-x values, respectively. For $x \simeq 0.25$ and at low temperatures a well-defined spin-glass region is observed. We propose that in this region there is a coexistence of a low-volume antiferromagnetic state and a high-volume ferromagnetic state with minima at the same energy as shown in Fig. 4(d). We now expect a low-temperature condensation of ferromagnetic Invar droplets and antiferromagnetic anti-Invar droplets. The observed spin-glass behavior is a direct consequence of this condensation.

VI. SUMMARY

To summarize, we use fixed-spin-moment spin-polarized total-energy band calculations to study the volume dependence of the magnetic behavior of transition metals and show that the total energy for certain systems must be represented by two separate branches corresponding to a low-spin (low-volume) state, and a high-spin (high-volume) state. We also show that, at the transition from nonmagnetic to magnetic behavior, the magnetic moment is unstable with respect to small volume changes and conclude that these systems exhibit magnetic instabilities. We find that these magnetic instabilities lie within the thermal range for fcc transition-metal systems with approximately 8.6 valence electrons/atom. That is, we note that there are two possible spin states at different energies and volumes. At low temperatures, only the low-energy state is excited. At some system-dependent temperature, lattice vibrations excite the

higher-lying state which has an effective rigid-lattice volume which is either less than or greater than that of the lower-lying state. As a consequence, there is either a pause or an enhancement in the thermal expansion.

We present fixed-spin-moment band calculations for Fe_3Ni and show that the zero-field energy versus volume for this ordered system has high-spin and low-spin branches which are separated by about 1 mRy, implying a characteristic Invar temperature of about 150 K. We further show that a common-tangent construction to the two branches implies that the high-spin and low-spin states are in equilibrium at a pressure of 55 kbar, and that magnetic collapse is expected at higher pressures.

We demonstrate that, at characteristic temperatures, Invar-like behavior is expected for electron concentrations greater than 8.6 and anti-Invar behavior is expected for concentrations less than 8.6. For iron rich alloys in the Fe-Ni system, we propose that the expected collapse in volume upon cooling may induce martensitic transformations, and we therefore identify our characteristic anti-Invar temperatures with the martensitic transformation temperatures. Near the critical electron concentration of 8.6 and at low temperatures, we expect complex magnetic behavior including dilute ferromagnetism and spin-glass behavior for Fe-Ni alloys. With the addition of manganese, chromium, or vanadium, the martensitic transformation is suppressed and the low-spin branch is antiferromagnetic so that a well-defined transition-metal spin-glass region should occur.

ACKNOWLEDGMENTS

I am indebted to M. Acet, P. M. Marcus, T. Penney, and E. F Wassermann for many helpful discussions on the Invar problem.

[1]C. E. Guillaume, C. R. Acad. Sci. **125**, 235 (1987).
[2]R. J. Weiss, Proc. Phys. Soc. **82**, 281 (1963).
[3]A. R. Williams, V. L. Moruzzi, C. D. Gelatt, Jr., and J. Kübler, J. Magn. Magn. Mater. **31-34**, 88 (1983).
[4]V. L. Moruzzi, Physica B **161**, 99 (1989).
[5]A. R. Williams, J. Kübler, and C. D. Gelatt, Jr., Phys. Rev. B **19**, 6096 (1976).
[6]A. R. Williams, V. L. Moruzzi, J. Kübler, and K. Schwarz, Bull. Am. Phys. Soc. **29**, 278 (1984).
[7]V. L. Moruzzi, P. M. Marcus, and P. C. Pattnaik, Phys. Rev. B **37**, 8003 (1988); V. L. Moruzzi and P. M. Marcus, *ibid.* **38**, 1613 (1988); V. L. Moruzzi and P. M. Marcus, J. Appl. Phys. **64**, 5598 (1988).
[8]V. L. Moruzzi, P. M. Marcus, K. Schwarz, and P. Mohn, Phys. Rev. B **34**, 1784 (1986).
[9]E. F. Wassermann, Adv. Solid State, **27**, 85 (1987).
[10]V. L. Moruzzi, J. F. Janak, and K. Schwarz, Phys. Rev. B **37**, 790 (1988).
[11]M. M. Abd-Elmeguid, B. Schleede, and H. Micklitz, J. Magn. Magn. Mater. **72**, 253 (1988); M. M. Abd-Elmeguid and H. Micklitz, Physica B **161**, 17 (1989).
[12]J. Crangle and G. C. Hallam, Proc. Phys. Soc. (London) **A272**, 119 (1963).
[13]L. Kaufman and M. Cohen, J. Met. **8**, 1393 (1956).
[14]M. Acet, H. Zähres, W. Stamm, and E. F. Wassermann, J. Appl. Phys. **63**, 3921 (1988).
[15]V. L. Moruzzi, P. M. Marcus, and J. Kübler, Phys. Rev. B **39**, 6957 (1989).
[16]H. Zähres, M. Acet, W. Stamm, and E. F. Wassermann, J. Magn. Magn. Mater. **72**, 80 (1988).
[17]T. Miyazaki, Y. Ando, and M. Takahashi, J. Magn. Magn. Mater. **60**, 219 (1986).
[18]V. L. Moruzzi, P. M. Marcus, and J. Kübler, Phys. Rev. B **39**, 6957 (1989).
[19]M. Shiga, T. Satake, Y. Wada, and Y. Nakamura, J. Magn. Magn. Mater. **51**, 123 (1985).